Journal of Geoscience and Environment Protection, 2023, 11, 96-105
https://www.scirp.org/journal/gep
ISSN Online: 2327-4344
ISSN Print: 2327-4336

Analyzing of the ENSO Index Using Extreme Value Theory

Fumio Maruyama

Department of Sports and Health Science, Matsumoto University, Matsumoto, Japan
Email: fmaruya@nagoya-u.jp

How to cite this paper: Maruyama, F. (2023). Analyzing of the ENSO Index Using Extreme Value Theory. *Journal of Geoscience and Environment Protection, 11,* 96-105.
https://doi.org/10.4236/gep.2023.116007

Received: April 30, 2023
Accepted: June 25, 2023
Published: June 28, 2023

Copyright © 2023 by author(s) and Scientific Research Publishing Inc.
This work is licensed under the Creative Commons Attribution International License (CC BY 4.0).
http://creativecommons.org/licenses/by/4.0/

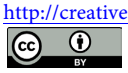

Open Access

Abstract

We predicted the extreme values of the ENSO index, the Niño3.4 index, and the Southern Oscillation Index (SOI) using extreme value theory. Various diagnostic plots for assessing the accuracy of the Generalized Pareto (GP) model fitted to the Niño3.4 index and SOI are shown, and all four diagnostic plots support the fitted GP model. Because the shape parameter of the Niño3.4 was negative, the Niño3.4 index had a finite upper limit. In contrast, that of the SOI was zero, therefore the SOI did not have a finite upper limit, and there is a possibility that a significant risk will occur. We predicted the maximum return level for the return periods of 10, 20, 50, 100, 350, and 500 years and their respective 95% confidence intervals, CI. The 10-year, and 100-year return levels for Niño3.4 were estimated to be 2.41, and 2.62, with 95% CI [2.22, 2.59], and [2.58, 2.66], respectively. The Niño3.4 index was 2.65 in the 2015/16 super El Niño, which is a phenomenon that occurs once every 500 years. The Niño3.4 index was 2.51 in the 1982/83, and 1997/98 super El Niño, which is a phenomenon that occurs once every 20 years. Recently, a large super El Niño event with a small probability of occurrence has occurred. In response to global warming, the super El Niño events are becoming more likely to occur.

Keywords

Extreme Value Theory, GP, ENSO, Niño3.4, SOI

1. Introduction

The Niño 3.4 index is the most commonly used index to define El Niño and La Niña events. The Southern Oscillation Index (SOI) is a standardized index based on the observed sea-level pressure differences between Tahiti and Darwin, Australia. The SOI measures the large-scale fluctuations in air pressure occurring between the western and eastern tropical Pacific during El Niño and La Niña ep-

isodes. Generally, the smoothed time series of the SOI corresponds well to changes in ocean temperatures across the eastern tropical Pacific. The negative phase of the SOI represents below-normal air pressure in Tahiti and above-normal air pressure in Darwin. Prolonged periods of negative (positive) SOI values coincide with abnormally warm (cold) ocean waters across the eastern tropical Pacific, which is typical of El Niño (La Niña) episodes.

Extreme value theory (EVT) has emerged as an important statistical discipline in applied science. Extreme value techniques are widely used in many other disciplines. For example, portfolio adjustment in the insurance industry, risk assessment in financial markets, and traffic prediction in telecommunications (Coles, 2001).

Statistical approaches focused on extreme values have shown promising results in unusual forecasting events in earth sciences, genetics, and finance. For instance, EVT was developed in the 1920s (Coles, 2001) and has been used to predict the occurrence of events, such as droughts and flooding (Katz et al., 2002) or financial crashes (Embrechts et al., 1997). Additionally, extreme value modeling has been applied in the fields of ocean wave modeling (Dawson, 2000), wind engineering (Harris, 2001), biomedical data processing (Roberts, 2000), earthquake thermodynamics (Alexandros et al., 2007), and public health (Thomas et al., 2016).

The monthly maximum rainfall data were modeled using the generalized extreme value models (Yin et al., 2014; Onwuegbuche et al., 2019). Zhang et al. (2010) fitted the generalized extreme value (GEV) distribution to the winter season maximum daily precipitation at many individual sites over North America with ENSO as a predictor of the parameters of the GEV distribution. This study predicts the extreme values of the Niño3.4 index, and SOI using the extreme value theory. An El Niño with particularly large amplitude is called super El Niño. A super El Niño disproportionately affects economies, societies, and ecosystems. Despite their importance, we do not fully understand how super El Niño develops its intensity and unique characteristics (Saji et al., 2018). The 2015 super El Niño event has been widely recognized as comparable to the 1982, and 1997 El Niño events (Ren et al., 2017). The observational analyses and modeling studies demonstrate that the principal difference between the 2015 and past super El Niño events lies in the exceptionally strong and consecutive occurrence of westerly wind burst events (Chen et al., 2017). Therefore, it is essential to predict super El Niño events.

2. Data and Method of Analysis

2.1. Data

The Niño3.4 index and SOI provided by NOAA's Climate Prediction Center, USA (CPC) were used. The monthly Niño3.4 index, which is a measure of the amplitude of an ENSO event, is defined as the monthly sea surface temperature (SST) averaged over the tropical Pacific areas (5˚N - 5˚S, 120˚ - 170˚W). The SOI is a standardized index based on the observed sea-level pressure differences

between Tahiti and Darwin, Australia. The negative (positive) SOI values coincide with abnormally warm (cold) ocean waters across the eastern tropical Pacific, which is typical of El Niño (La Niña) episodes.

2.2. Extreme Value Theory

2.2.1. Generalized Pareto (GP) Distributions

The modeling only block maxima is a wasteful approach to extreme value analysis if other data on extremes are available. In this technique, the data are collected over a specific threshold value. Modeling the extremes using this method enables a more efficient usage of extreme value information than that given by an analysis of annual maxima data, which excludes many extreme events that did not happen to be the largest annual event. In this study, the data were fitted to the GP distribution:

$$G(z)=1-\left[1+\xi\left(\frac{z-u}{\sigma}\right)\right]^{-1/\xi}, \text{ for } \xi\neq 0,$$

$$G(z)=1-\exp\left(-\left(\frac{z-u}{\sigma}\right)\right), \text{ for } \xi=0, \quad (1)$$

where z is the extreme value from the blocks, u is the known threshold, σ is the scale parameter, and ξ is the shape parameter.

2.2.2. Return Levels

The level of return for the GP distribution is formed by the geometric locations of the points (m, x_m) for large values of m, where x_m is the return level estimated from the m-observation:

$$x_m=u+\frac{\sigma}{\xi}\left[(m\zeta_u)^{\xi}-1\right], \text{ for } \xi\neq 0,$$

$$x_m=u+\sigma\log(m\zeta_u), \text{ for } \xi=0, \quad (2)$$

where u is the selected threshold value, $\zeta_u=\Pr(x>u)=k/n$, k is the number of exceedances, and n is the number of observations.

Modeling was performed using the evd package in R for GP distribution calculations. Because we want to know how small the value will be as a strong El Niño event, we need to multiply the SOI data by –1 to put it in the framework of extremum statistics that considers the maximum.

3. Results

3.1. Niño3.4 Index

The Niño3.4 index is shown in Figure 1. Figure 2 shows the wavelet power spectrum of the Niño3.4 index. For 1980-1990, a strong priority over four years was observed.

Table 1 shows the results of the GP modeling on the Niño3.4 index. The model has the scale parameter, σ, and shape parameter, ξ. Because ξ is negative, the Niño3.4 index has a finite upper limit.

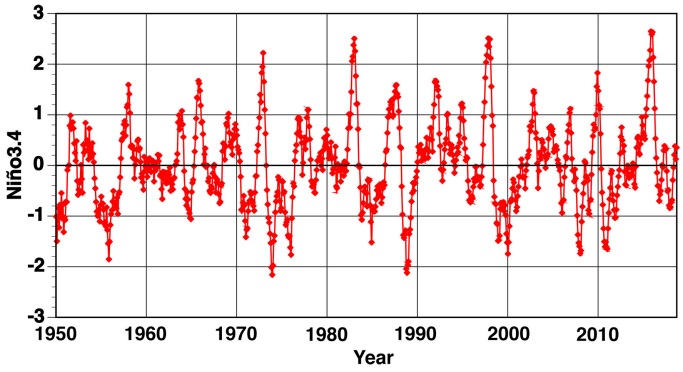

Figure 1. Plot of the Niño3.4 index.

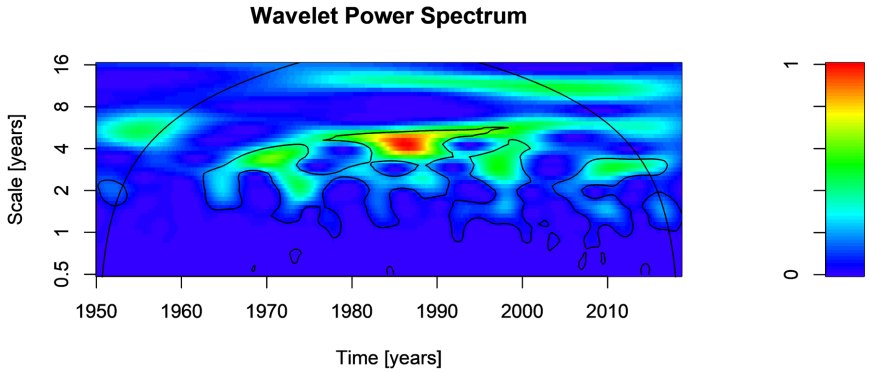

Figure 2. Wavelet power spectrum of the Niño3.4.

Table 1. GP parameter estimates for the Niño3.4.

	σ	ξ
Parameter estimate	1.02	−0.880
Standard errors	0.213	0.196
95% CI	[0.599, 1.43]	[−1.26, −0.496]

Table 2 shows the predicted maximum return levels for the return periods of 10, 20, 50, 100, 350, and 500 years and their respective 95% confidence intervals, CI. The 10-year return level was estimated to be 1.12, with 95% CI [1.04, 1.21]. The 100-year return level was estimated to be 2.13, with 95% CI [1.97, 2.30]. Another way to interpret the plot is to say that there is an approximately 1% chance (1/100) each year that the Niño3.4 index will exceed 2.13. There is an approximately 10% chance (1/10) each year that the Niño3.4 index will exceed 1.12.

Various diagnostic plots for the fitted GP distributions are shown in Figure 3. Straight lines and curves represent the estimated functions. Each point plot represents a realization value. The lines on both sides represent the 95% CI. The output provides little reason to doubt the validity of the GP model. Neither the probability plot nor the quantile plot doubts the validity of the fitted model: each

set of plotted points is near-linear. In the return level curve, the estimated curve is not linear because ξ is not close to zero. Finally, the corresponding density estimates are consistent with the data. Consequently, all four diagnostic plots support the fitted GP model. Because there were 39 exceedances of the threshold u = 1.5 in the complete set of 840 observations, the maximum likelihood estimate of the exceedance probability was 0.0473.

3.2. SOI

The SOI is shown in Figure 4. Figure 5 shows the wavelet power spectrum of the SOI. For 1980-1990, a strong priority of four years was observed.

Table 2. GP return level estimates for the Niño3.4.

Return period (year)	10	20	50	100	350	500
Return level	2.41	2.52	2.59	2.62	2.64	2.65
Standard errors	0.0935	0.0621	0.0305	0.0186	0.0181	0.0193
95% CI	[2.22, 2.59]	[2.40, 2.64]	[2.53, 2.65]	[2.58, 2.66]	[2.61, 2.68]	[2.61, 2.68]

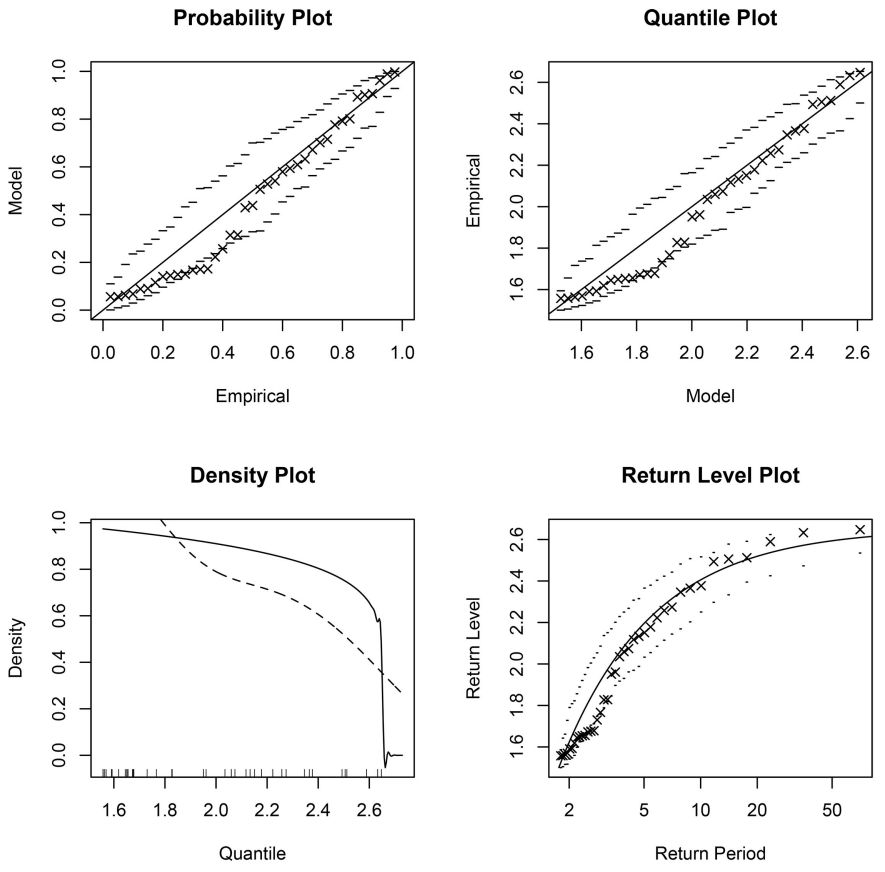

Figure 3. Diagnostic plots for threshold excess model fitted to the Niño3.4 during the period 1950-2019.

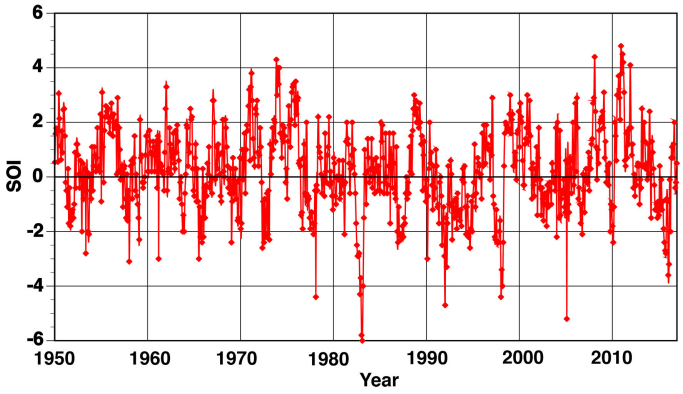

Figure 4. The plot of the SOI.

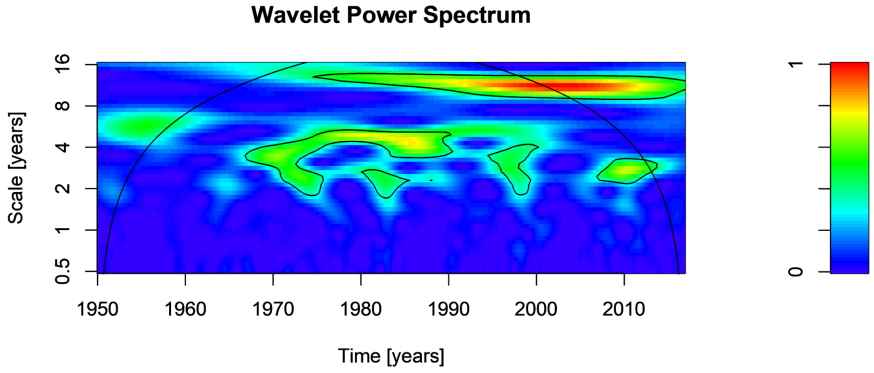

Figure 5. Wavelet power spectrum of the SOI.

Table 3 shows the results of GP modeling on the SOI. ξ was close to zero (0.0402) and included zero as a confidence interval. Therefore, the SOI does not have a finite upper limit. Table 4 shows the predicted maximum return levels for the return periods of 10, 20, 50, 100, 350, and 500 years and their respective 95% CI. The 10-year return level was estimated to be −3.94, with 95% CI [−4.48, −3.41]. The 100-year return level was estimated to be −6.26, with 95% CI [−8.49, −4.03].

The various diagnostic plots for the fitted GPD are shown in Figure 6. The output gives little reason to doubt the validity of the GP model. Neither the probability plot nor the quantile plot doubts the validity of the fitted model: each set of plotted points is near-linear. Furthermore, the estimated curve in the return level curve is linear because ξ is close to zero. Finally, the corresponding density estimate is consistent with the data. Consequently, all the four diagnostic plots supported the fitted GP model. Because there were 44 exceedances of the threshold u = 2.2 in the complete set of 804 observations, the maximum likelihood estimate of the exceedance probability was 0.0548.

4. Discussion

The return level at each return period for Niño3.4 is shown in Figure 7. In the case of ξ < 0, for the Niño3.4, the plots deviated from a straight line and were

convex upward. According to the Niño3.4 index, the super El Niño was the largest in the 2015/16, followed by the 1982/83, and 1997/98 El Niño events. In the 2015/16 case, the amplitude and area of a negative horseshoe-shaped sea surface temperature (SST) anomaly in the Pacific Ocean were the smallest in the three cases, and a negative SST anomaly in the Philippine Sea was weaker than in the previous two cases (Shiozaki & Enomoto, 2020). The Niño3.4 index was 2.65 in the 2015/16 super El Niño, which is a phenomenon that occurs once every 500 years, because the 500-year return level was 2.65 (Table 2). The Niño3.4 index was 2.51 in the 1982/83, and 1997/98 super El Niño, which is a phenomenon that occurs once every 20 years, as shown in Table 2. In response to global warming, the super El Niño events are becoming more likely to occur.

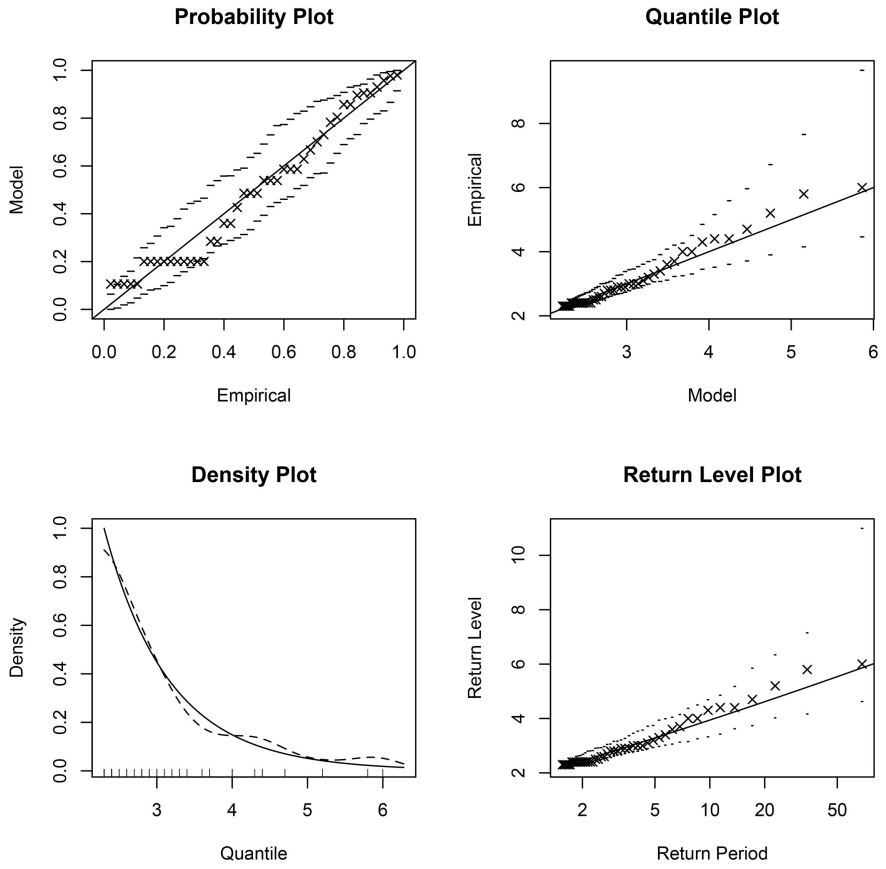

Figure 6. Diagnostic plots for threshold excess model fitted to the SOI during the period 1950-2019.

Table 3. GP parameter estimates for the SOI.

	σ	ξ
Parameter estimate	0.890	0.0402
Standard errors	0.221	0.197
95% CI	[0.457, 1.32]	[−0.347, 0.427]

Table 4. GP return level estimates for the SOI.

Return period (year)	10	20	50	100	350	500
Return level	−3.94	−4.62	−5.54	−6.26	−7.61	−8.01
Standard errors	0.273	0.411	0.748	1.14	2.14	2.50
95% CI	[−4.48, −3.41]	[−5.42, −3.81]	[−7.06, −4.07]	[−8.49, −4.03]	[−11.8, −3.41]	[−12.9, −3.10]

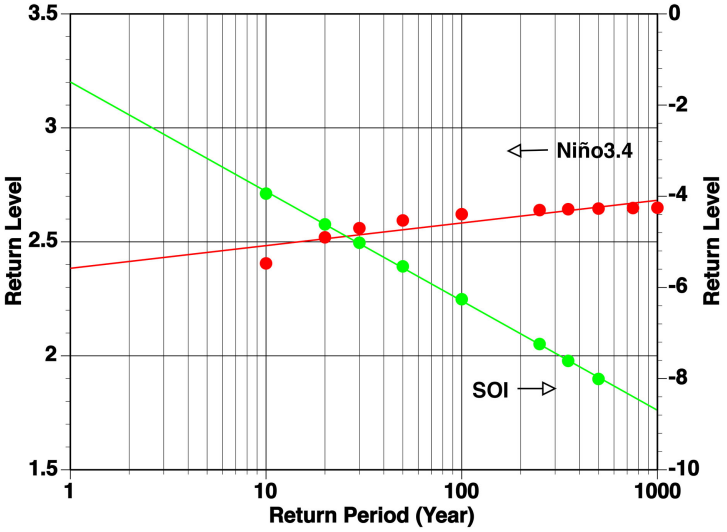

Figure 7. Return level plot for the Niño3.4 and SOI.

Figure 7 also shows the return level for each return period for the SOI. It increased significantly, which corresponded to have no upper limit in the case of ξ = 0. The $\xi = 0$ case exhibited a heavy-tailed distribution. In the ξ = 0 case, the upper limit is infinite, therefore there is a possibility that a significant risk will occur. According to the SOI, the super El Niño was the largest in the 1982/83, followed by the 1997/98, and 2015/16 cases. The SOI in the 2015/16 El Niño was large, because the Walker circulation was weakened in narrower zonal extent owing to the westernmost positive SST anomaly in the eastern Pacific Ocean than in the 1982/83, and 1997/98 El Niño (Shiozaki & Enomoto, 2020). The SOI was −3.6 in the 2015/16 super El Niño, which is a phenomenon that occurs once every 10 years, is shown in Table 2. The SOI were −6 and −4.4 in the 1982/83, and 1997/98 super El Niño, respectively, which is a phenomenon that occurs once every 100, and 20 years, as shown in Table 4.

5. Conclusion

We predicted the extreme values of the Niño3.4 index and SOI using the extreme value theory. The main findings are summarized as follows:

1) Various diagnostic plots for assessing the accuracy of the GP model fitted to the Niño3.4 index and SOI are shown, and all four diagnostic plots support the fitted GP model. Because the shape parameter of the Niño3.4 was negative, the Niño3.4 index had a finite upper limit. In contrast, that of the SOI was zero,

so the SOI did not have a finite upper limit, and there is a possibility that a significant risk will occur.

2) We predicted the maximum return level for the return periods of 10, 20, 50, 100, 350, and 500 years along with their respective 95% confidence intervals. As a result, the 10-year and 100-year return levels for Niño3.4 were estimated to be 2.41 and 2.62, with 95% CI [2.22, 2.59], and [2.58, 2.66], respectively.

3) The Niño3.4 index was 2.65 in the 2015/16 super El Niño, which is a phenomenon that occurs once every 500 years. The Niño3.4 index was 2.51 in the 1982/83, and 1997/98 super El Niño, which is a phenomenon that occurs once every 20 years. Recently, a large super El Niño with small probability of occurrence has occurred. In response to global warming, super El Niño events are becoming more likely to occur.

We want to make more accurate super El Niño predictions.

4) The return level at each return period for the Niño3.4 deviated from the straight line and was convex upward, corresponding to having an upper limit in the case of $\xi < 0$. On the other hand, that of SOI increased cleanly, and it corresponded to having no upper limit in the case of $\xi = 0$.

Conflicts of Interest

The author declares no conflicts of interest regarding the publication of this paper.

References

Alexandros, A. Z., Nickolaos, E. F., & Athanasios, A. P. (2007). Modeling Earthquake Risk via Extreme Value Theory and Pricing the Respective Catastrophe Bonds. *ASTIN Bulletin, 37,* 163-183. https://doi.org/10.2143/AST.37.1.2020804

Chen, L., Li, T., Wang, B., & Wang, L. (2017). Formation Mechanism for 2015/16 Super El Niño. *Scientific Reports, 7,* Article No. 2975. https://doi.org/10.1038/s41598-017-02926-3

Coles, S. (2001). *An Introduction to Statistical Modeling of Extreme Values*. Springer-Verlag. https://doi.org/10.1007/978-1-4471-3675-0

Dawson, T. H. (2000). Maximum Wave Crests in Heavy Seas. *Journal of Offshore Mechanics and Arctic Engineering-Transactions of the AMSE, 122,* 222-224. https://doi.org/10.1115/1.1287039

Embrechts, P., Klüppelberg, C., & Mikosch, T. (1997). *Modeling Extremal Events for Insurance and Finance*. Springer-Verlag. https://doi.org/10.1007/978-3-642-33483-2

Harris, R. I. (2001). The Accuracy of Design Values Predicted from Extreme Value Analysis. *Journal of Wind Engineering and Industrial Aerodynamics, 89,* 153-164. https://doi.org/10.1016/S0167-6105(00)00060-X

Katz, R. W, Parlange, M. B., & Naveau, P. (2002). Statistics of Extremes in Hydrology. *Advances in Water Resources, 25,* 1287-304. https://doi.org/10.1016/S0309-1708(02)00056-8

Onwuegbuche, F. C., Kenyatta, A. B., Affognon, S. B., Enock, E. P., & Akinade, M. O. (2019). Application of Extreme Value Theory in Predicting Climate Change Induced Extreme Rainfall in Kenya. *International Journal of Statistics and Probability, 8,* 85-94.

https://doi.org/10.5539/ijsp.v8n4p85

Ren, H. L., Wang, R., Zhai, P., Ding, Y., & Lu, B. (2017). Upper-Ocean Dynamical Features and Prediction of the Super El Nino in 2015/16: A Comparison with the Cases in 1982/83 and 1997/98. *Journal of Meteorological Research, 31,* 278-294. https://doi.org/10.1007/s13351-017-6194-3

Roberts, S. J. (2000). Extreme Value Statistics for Novelty Detection in Biomedical Data Processing. *IEE Proceedings—Science Measurement and Technology, 147,* 363-367. https://doi.org/10.1049/ip-smt:20000841

Saji, N. H., Jin, D., & Thilakan, V. (2018). A Model for Super El Ninos. *Nature Communications, 9,* 2528-2515. https://doi.org/10.1038/s41467-018-04803-7

Shiozaki, M., & Enomoto, T. (2020). Comparison of the 2015/16 El Niño with the Two Previous Strongest Events. *SOLA, 16,* 12-16. https://doi.org/10.2151/sola.2020-003

Thomas, M., Lemaitre, M., Wilson, M. L., Vibound, C., Yordanov, Y., Wackernagel, H., & Carrat, F. (2016). Applications of Extreme Value Theory in Public Health. *PLOS ONE, 11,* e0159312. https://doi.org/10.1371/journal.pone.0159312

Yin, Y., Xu, C. Y., Chen, H., Li, L., Li, H., & Xu, H. (2014). Modeling the Extreme Precipitation Using the Generalized Extreme Value Models with Southern Oscillation Index (SOI) as a Covariate in the Beas Basin, India. *Geophysical Research Abstracts, 16,* EGU2014-6751.

Zhang, X., Wang, J., Zwiers, F. W., & Groisman, P. Y. (2010). The Influence of Large Scale Climate Variability on Winter Maximum Daily Precipitation over North America. *Journal of Climate, 23,* 2902-2915. https://doi.org/10.1175/2010JCLI3249.1